RESEARCH ARTICLE

The Peptidoglycan-Binding Protein SjcF1 Influences Septal Junction Function and Channel Formation in the Filamentous Cyanobacterium *Anabaena*

Mareike Rudolf,[a] Nalan Tetik,[a] Félix Ramos-León,[b] Nadine Flinner,[a,c] Giang Ngo,[a] Mara Stevanovic,[a] Mireia Burnat,[b] Rafael Pernil,[b] Enrique Flores,[b] Enrico Schleiff[a,c,d]

Institute for Molecular Biosciences, Goethe University, Frankfurt, Germany[a]; Instituto de Bioquímica Vegetal y Fotosíntesis, CSIC and Universidad de Sevilla, Seville, Spain[b]; Cluster of Excellence Macromolecular Complexes[c] and Buchman Institute for Molecular Life Sciences[d], Goethe University, Frankfurt, Germany

ABSTRACT Filamentous, heterocyst-forming cyanobacteria exchange nutrients and regulators between cells for diazotrophic growth. Two alternative modes of exchange have been discussed involving transport either through the periplasm or through septal junctions linking adjacent cells. Septal junctions and channels in the septal peptidoglycan are likely filled with septal junction complexes. While possible proteinaceous factors involved in septal junction formation, SepJ (FraG), FraC, and FraD, have been identified, little is known about peptidoglycan channel formation and septal junction complex anchoring to the peptidoglycan. We describe a factor, SjcF1, involved in regulation of septal junction channel formation in the heterocyst-forming cyanobacterium *Anabaena* sp. strain PCC 7120. SjcF1 interacts with the peptidoglycan layer through two peptidoglycan-binding domains and is localized throughout the cell periphery but at higher levels in the intercellular septa. A strain with an insertion in *sjcF1* was not affected in peptidoglycan synthesis but showed an altered morphology of the septal peptidoglycan channels, which were significantly wider in the mutant than in the wild type. The mutant was impaired in intercellular exchange of a fluorescent probe to a similar extent as a *sepJ* deletion mutant. SjcF1 additionally bears an SH3 domain for protein-protein interactions. SH3 binding domains were identified in SepJ and FraC, and evidence for interaction of SjcF1 with both SepJ and FraC was obtained. SjcF1 represents a novel protein involved in structuring the peptidoglycan layer, which links peptidoglycan channel formation to septal junction complex function in multicellular cyanobacteria. Nonetheless, based on its subcellular distribution, this might not be the only function of SjcF1.

IMPORTANCE Cell-cell communication is central not only for eukaryotic but also for multicellular prokaryotic systems. Principles of intercellular communication are well established for eukaryotes, but the mechanisms and components involved in bacteria are just emerging. Filamentous heterocyst-forming cyanobacteria behave as multicellular organisms and represent an excellent model to study prokaryotic cell-cell communication. A path for intercellular metabolite exchange appears to involve transfer through molecular structures termed septal junctions. They are reminiscent of metazoan gap junctions that directly link adjacent cells. In cyanobacteria, such structures need to traverse the peptidoglycan layers in the intercellular septa of the filament. Here we describe a factor involved in the formation of channels across the septal peptidoglycan layers, thus contributing to the multicellular behavior of these organisms.

Cyanobacteria are Gram-negative bacteria with a cell envelope composed of a plasma membrane, a peptidoglycan (PG) layer, and an outer membrane, where the latter two are often referred to as the cell wall with the space between the plasma and the outer membranes referred to as the periplasm. Some cyanobacteria, such as *Anabaena* sp. strain PCC 7120 (here *Anabaena*) are filamentous, growing as chains of cells, including vegetative cells, active in oxygenic photosynthesis-dependent CO_2 fixation, and heterocysts. The latter are specialized cells for nitrogen fixation and are formed from vegetative cells under nitrogen deprivation (1). The outer membrane of filamentous cyanobacteria does not enter the septum between

two consecutive cells (2–5). In contrast, the A1-type PG layer (6) surrounds each cell in the filament (7), while the layers of adjacent cells might interact in the septum (8). The width of the PG layer is about 12 nm (7), and PG in *Anabaena* is composed of more than one layer (9). Remarkably, polysaccharides composed of glucosamine, mannosamine, galactosamine, mannose, and glucose are covalently linked to the PG of cyanobacteria, as shown for the unicellular *Synechocystis* sp. strain PCC 6714 (10), a property typical for Gram-positive bacteria. However, the degree of covalent cross-links between PG chains is rather comparable to that in Gram-negative bacteria (9). These observations led to the proposal that cells of *Anabaena* are like

unicellular Gram-positive bacteria with a plasma membrane and a thick PG layer arranged in an outer membrane sack (7).

The continuous outer membrane determines the presence of a continuous periplasm, which has been discussed to allow exchange of molecules along the filament, as exemplified by the green fluorescent protein (GFP) (11). Since the periplasm is thought to form a gel-like texture (12), it would represent one possible route for metabolite exchange or signaling between heterocysts and vegetative cells (9, 11). However, the continuous nature of the periplasmic space has been questioned (13). From the structural point of view, the PG layer might represent a barrier that slows down movement of molecules as large as GFP but perhaps not of small molecules, such as some metabolites (7, 11).

An alternative mode for intercellular molecular exchange might involve septal junction complexes (14), also termed microplasmodesmata, septosomes, or "channels connecting cells," which have been identified between cells of filamentous cyanobacteria (e.g., see references 7 and 15–18). The size of the inner diameter of the septal junction complexes was determined by potassium permanganate staining and is about 6 nm (7). Proteins involved in septal junction complex formation have been classified as "cell-cell joining" proteins, and mutants of the corresponding genes show a filament fragmentation phenotype (5, 19, 20). Today, the SepJ (also known as FraG [19, 20]), FraC, and FraD (5, 21, 22) proteins have been identified as possible components of septal junction complexes.

Recently, the question concerning integration of the PG layer and septal junction complex formation has been addressed. If septal junction proteins from adjacent cells interact with each other, they should traverse the septal PG layer(s). The presence of perforations, also termed nanopores, in septal PG discs has been demonstrated for *Nostoc punctiforme* recently (23). The periplasmic amidase AmiC2 has been shown to be involved in the formation of such structures (23). Based on cell-cell communication analysis, an ortholog of AmiC2 in *Anabaena*, encoded by *alr0092* and annotated AmiC1, has also been found to influence septal junction formation (24). Thus, those perforations can be the channels through which septal junction complexes traverse the septal PG. However, a possible regulation of the dimension of the septal junction channel is unknown. Here we describe a further protein factor encoded by *all1861* that influences septal junction channel formation in *Anabaena*. This factor restricts the size of the channels in the PG layer, leading to its annotation as peptidoglycan septal junction channel formation protein no. 1 (SjcF1).

RESULTS

SjcF1 proteins are present in filamentous cyanobacteria. SjcF1 encoded by *sjcF1* (*all1861*) was found in the proteomic analysis of cell wall fractions from *Anabaena* (25, 26). The gene is the last one of a gene cluster (Fig. 1A; see Fig. S1 in the supplemental material). It encodes a protein with a transmembrane segment (not shown in Fig. 1B), an SH3 domain, known to be involved in protein-protein interactions (27), and two PG binding domains (Fig. 1B). The occurrence of the gene in such a genomic organization is limited to *Anabaena* and *Anabaena variabilis*, while the corresponding gene in *Nostoc punctiforme*, a related cyanobacterium, is downstream of a gene coding for a response regulator/receiver protein (Fig. 1A). A global search for proteins with similar domain architecture showed its presence in 12 organisms in addition to *Anabaena* (see Table S1 in the supplemental material). Only in
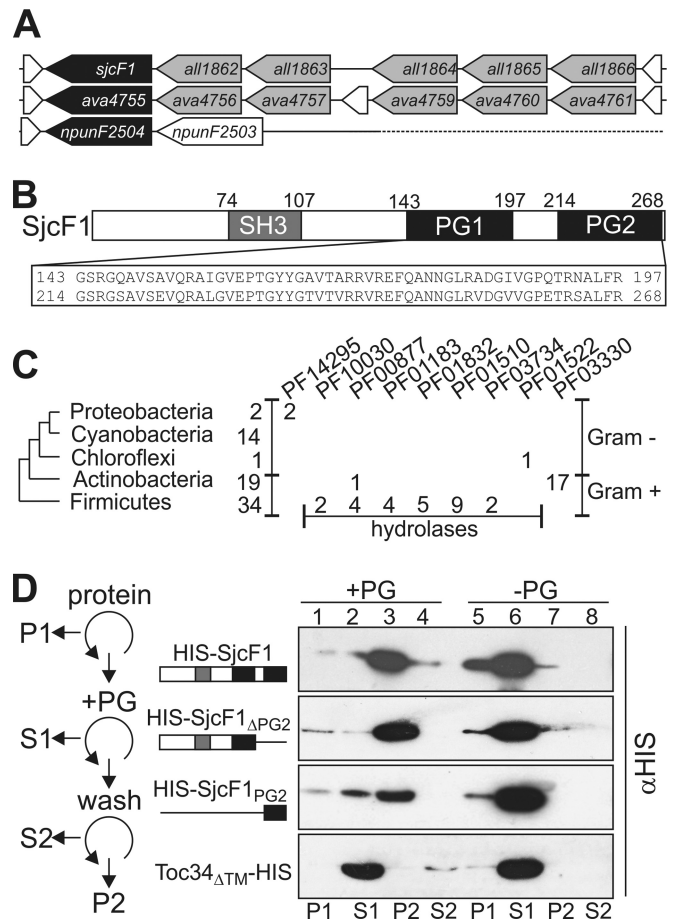
FIG 1 SjcF1 interacts with peptidoglycan. (A) Genomic organization of *sjcF1* (*Anabaena*) and its homologues *ava4755* (*Anabaena variabilis*) and *npunF2504* (*Nostoc punctiforme*). Gray indicates genes with comparable sequence in *Anabaena* and *A. variabilis*. Genes indicated in white are distinct between the three species. For clarity, only one succeeding gene of *Nostoc punctiforme* is shown. (B) Functional domains for SjcF1 are indicated. (C) The numbers of sequences containing an SH3 domain (PF08239) and a PG binding domain (PF01471) (first column) and the numbers of additional domains (next columns [Pfam code]) are given. Taxonomic groups where no sequences are identified are excluded. (D) His-tagged SjcF1 (top), SjcF1 without the 2nd PG binding domain (2nd panel), the 2nd PG binding domain of SjcF1 (3rd panel), or Toc34ΔTM (bottom panel) were centrifuged (lane 1, pellet P1), and supernatant was incubated with PG (+PG), After centrifugation (lane 2, supernatant S1), the pellet was washed and centrifuged (lanes 3 and 4, pellet P2 and supernatant S2, respectively). Proteins were subjected to SDS-PAGE and immunodecorated with anti-His tag. Lanes 5 to 8 show the experiment without addition of PG. The experimental scheme is shown on the left.

Spirulina subsalsa were two forms identified. All cyanobacteria with such a protein are multicellular and filamentous. We also identified sequences containing both domains characterizing SjcF1 in Gram-positive *Actinobacteridae* (Fig. 1C), but they contain a "rare lipoprotein A-like double-psi β-barrel" (Pfam, DPBB_1 [28]) not found in SjcF1. Moreover, 34 sequences from Gram-positive bacteria of the phylum *Firmicutes* were identified, again mostly with additional domains characteristic for hydrolases. Thus, a protein with the molecular architecture of SjcF1 is specific for filamentous cyanobacteria, but in Gram-positive bacteria that have a thick PG layer, proteins with a similar but not identical domain architecture to that of SjcF1 exist, which might fulfill similar functions.

The peptidoglycan binding domain of SjcF1 is functional. The functionality of the predicted PG binding domains needed experimental confirmation (Fig. 1D). We isolated PG from *Anabaena* and heterologously expressed SjcF1 with an N-terminal His tag (Materials and Methods). SjcF1 binding to PG was analyzed by incubation of the soluble recombinant protein with purified PG, and the bound protein was recovered by centrifugation (P2, lane 3). We observed that SjcF1 binds to PG (upper panel), because it pellets in the presence (lane 3) but not in the absence of PG (lane 7). The same result was observed for a variant of the protein not containing PG2 (SjcF1$_{\Delta PG2}$) or consisting of PG2 only (SjcF1$_{PG2}$; lane 3 versus lane 7). The specificity was further confirmed by the absence of an interaction between PG and the chloroplast translocon component Toc34, used as a negative control (29). We conclude that SjcF1 directly interacts with the PG layer.

***sjcF1* is expressed in an environmentally controlled manner.** The transcript abundance of *sjcF1* was estimated by reverse transcription (RT)-PCR. We observed a transcript in cells grown in BG11 medium suggesting that *sjcF1* is expressed under standard growth conditions (Fig. 2A, lane 1). However, the transcript abundance was reduced upon nitrogen starvation (lanes 2 and 3), although it recovered to some extent 12 h after nitrogen step down (lanes 4 and 5). To investigate whether *sjcF1* expression is reduced in heterocysts, which comprise about 5 to 10% of all cells in the filament (1), we created the strain AFS-PDGF-*sjcF1*, in which the GFP gene is fused to a 740-bp fragment of the 5′ end and upstream region of *sjcF1*, including in frame its start codon (Table 1). This construct was incorporated into a neutral site of the *Anabaena* genome, the *nucA-nuiA* region of the α megaplasmid (see Materials and Methods). GFP fluorescence was observed within the cytoplasm of vegetative cells, whereas it was reduced in heterocysts (Fig. 2B). Quantification revealed that the fluorescence intensity in heterocysts was on average about half of the one found in vegetative cells (Fig. 2C). These observations suggest that *sjcF1* expression is dependent on environmental conditions. To explore this further, we incubated *Anabaena* in BG11 medium with different compositions (Fig. 2D). Again the overall expression after growth in BG11$_0$ medium (which lacks combined nitrogen) was reduced compared to that in cells grown in BG11 medium (bar 1). Exclusion of copper, iron, zinc, or citric acid from the growth medium (bars 2 to 5) did not result in a significant change of transcript levels. In contrast, an enhanced copper concentration (5 μM [a 16-fold higher concentration than in BG11]) resulted in a moderate increase, and an enhanced iron (1 mM [45-fold higher than in BG11]) or zinc (5 μM [7-fold higher than in BG11]) content enforced an at least 4-fold increase of transcript abundance (bars 6 to 8). It is known that PG can bind metals with an affinity order of Zn > Fe(III) > Cu (30, 31), and that an excess of such metals leads to PG damage (32). Thus, the observed transcript enrichment under elevated metal concentration is consistent with the hypothesis that SjcF1 is involved in PG maintenance by yet to be discovered means.

SjcF1 affects the cell wall integrity. We generated an insertional mutant of *sjcF1*, strain AFS-I-*sjcF1* (Materials and Methods) (Table 1). Southern blot analysis of three independently generated mutant clones and PCR on genomic DNA (see Fig. S1 in the supplemental material) indicated that chromosomes bearing the insertion were not fully segregated. The heterozygous mutant did not show a growth delay in BG11 medium or a Fox⁻ phenotype (see Fig. S1 in the supplemental material). Guided by the observed
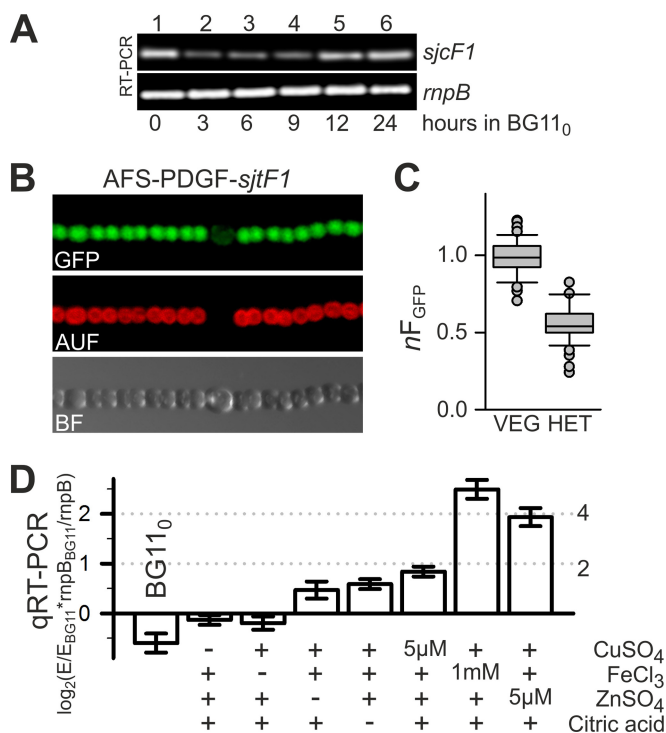

FIG 2 SjcF1 is differentially expressed in different cell types and growth media. (A) mRNA was isolated from *Anabaena* cells grown in BG11 medium and incubated for the indicated times in BG11$_0$ medium, and RT-PCR was performed to amplify *sjcF1* (top panel) and *rnpB*, used as a control (bottom panel). (B) In strain AFS-PDGF-*sjcF1*, *gfp* is expressed from the *sjcF1* promoter. GFP fluorescence, cyanobacterial autofluorescence, and the bright-field image are shown for a representative filament grown for 24 h in BG11$_0$. (C) Average GFP fluorescence from vegetative cells of AFS-PDGF-*sjcF1* was used for normalization of fluorescence of individual vegetative cells and heterocysts of the same filament. The box plot shows the normalized fluorescence of vegetative cells ($n > 80$) and heterocysts ($n = 11$) from 8 individual filaments. The difference is significant (t test, $P < 0.001$). (D) mRNA abundance of *sjcF1* after 7 days of growth under various conditions was analyzed by qRT-PCR and normalized to the expression in BG11 and the expression of *rnpB*. Results are averages of ≥3 biological independent replicas (E, expression of *sjcF1*). The fold change is given on the right. +, presence in typical concentrations; −, BG11 preparation without the indicated substance.

PG binding capacity of SjcF1, we investigated the impact of the mutation on cell wall integrity. We analyzed the growth of AFS-I-*sjcF1* in the presence of compounds known to affect growth, depending on cell wall integrity (Fig. 3A) (33). A strain with a mutation in the lipid A synthesis gene *alr2270* (AFS-I-*alr2270*) (33) and two control strains (AFS-I-P24 and CSR10; which bear sequences including the C.S3 cassette inserted in unrelated genes [Table 1]) were included in the analysis. For AFS-I-*alr2270* and AFS-I-*sjcF1*, but not for the control strains, we observed a drastic growth reduction in the presence of SDS (Fig. 3A, panel ii) or ampicillin (panel iv). However, for AFS-I-*sjcF1*, the sensitivity toward lysozyme was not as drastic as in AFS-I-*alr2270* (panel iii). This suggests that in AFS-I-*sjcF1*, outer membrane integrity is affected, but not in the same manner as by altering lipid A synthesis, as previously described (33). Consistently, the overall lipid content of the mutant was not changed compared to that in control cells (see Fig. S1 in the supplemental material).

SjcF1 is not involved in the general PG synthesis. We aimed at PG staining with a fluorescent derivative of vancomycin (Van-FL)

TABLE 1 *Anabaena* strains used in this study

| Strain	Resistance	Genotype	Properties	Reference
Anabaena sp. strain PCC 7120		Wild type		C. P. Wolk
CSR10	Sp^r Sm^r	*alr4167*::pCSV3	Gene interruption by pCSV3 plasmid	52
AFS-I-P24	Sp^r Sm^r	*alr7361-alr7362*::pCSEL24	Gene interruption by pCSEL24 plasmid	55
AFS-I-*sjcF1*	Sp^r Sm^r	*all1861*::pCSV3	Gene interruption by pCSV3 plasmid	This study
AFS-I-2270	Sp^r Sm^r	*alr2270*::pCSV3	Gene interruption by pCSV3 plasmid	33
CSR27	Sp^r Sm^r	*alr2458*::pCSV3	Gene interruption by pCSV3 plasmid	This study
CSVM34		Δ*sepJ*	Gene deletion	71
CSVT1		Δ*fraC*	Gene deletion	21
CSVM141		Δ*sepJ* Δ*fraC* Δ*fraD*	Gene deletion	40
AFS-PDGF-*sjcF1*	Sp^r Sm^r	P$_{all1861}$-*gfp* in *nucA-nuiA* region	*all1861* promoter-GFP fusion	This study
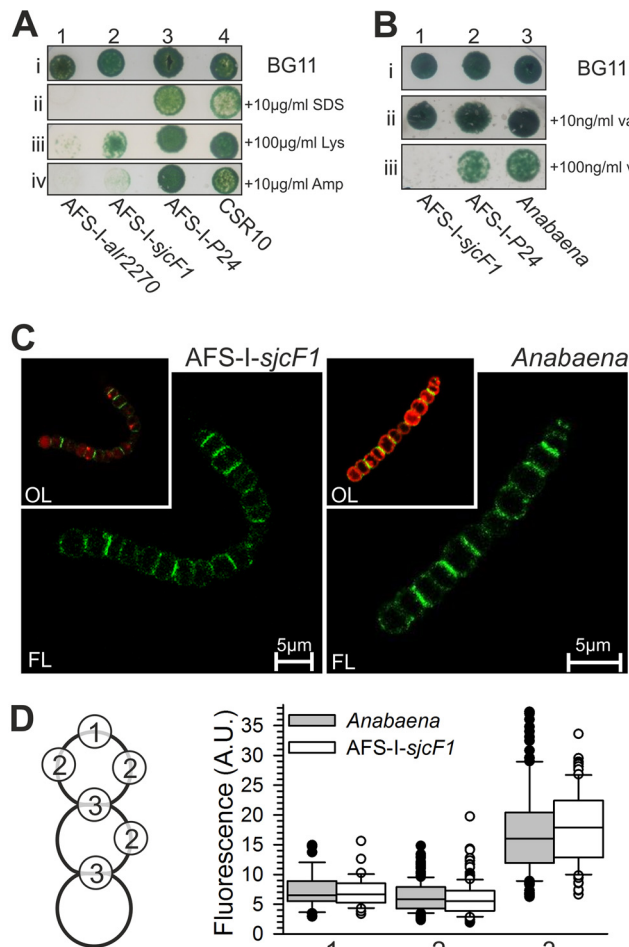
FIG 3 AFS-I-*sjcF1* has an altered cell wall functionality. (A) Growth of AFS-I-*alr2270* (lane 1), AFS-I-*sjcF1* (lane 2), AFS-I-P24 (lane 3), and CSR10 (lane 4) on BG11 plates (i) with 10 μg/ml SDS (ii), 100 μg/ml lysozyme (iii), or 10 μg/ml ampicillin (iv) was inspected after 7 days of incubation. (B) Growth of AFS-I-*sjcF1* (lane 1), AFS-I-P24 (lane 2), and *Anabaena* sp. strain PCC 7120 (lane 3) on BG11 plates (i) with 10 (ii) or 100 (iii) ng/ml vancomycin was inspected after 7 days of incubation. (C) AFS-I-*sjcF1* or *Anabaena* cells grown in BG11 medium incubated with Van-FL were analyzed by confocal laser scanning microscopy (CLSM). Shown is fluorescence of Van-FL (FL) and overlay with autofluorescence (OL). Controls are shown in Fig. S2 in the supplemental material. (D) Van-FL fluorescence at defined cell positions (left) of individual cells of ≥15 different filaments of *Anabaena* (gray) and AFS-I-*sjcF1* (white) recorded with identical settings was quantified. A.U., arbitrary units.

to explore the impact of SjcF1 on PG synthesis (23, 34). We realized that AFS-I-*sjcF1* is more sensitive to vancomycin than the wild-type strain (Fig. 3B), as growth of the insertional mutant, but not of the control strain AFS-I-P24 or the wild type, was drastically reduced in the presence of 100 ng/ml vancomycin (panel iii). Subsequently we inspected the incorporation of Van-FL into the PG layer (Fig. 3C). We observed staining for both AFS-I-*sjcF1* and the *Anabaena* wild type, and quantification of the incorporated Van-FL yielded very similar distributions for both strains (Fig. 3D). As expected from the juxtaposition of the two PG layers, a 2-fold-higher fluorescence intensity was observed at the cell-cell contact sides (position 3) compared to the filament ends (position 1) or cell sides (position 2) (Fig. 3D).

Next we inactivated the *alr2458* gene encoding an alanine racemase putatively involved in PG biosynthesis to judge whether SjcF1 is related to PG synthesis by comparison of the mutant phenotypes (Fig. 4A). Segregation of the insertional mutant of *alr2458*, strain CSR27, was analyzed by PCR on genomic DNA (Fig. 4A and B). A faint band in strain CSR27 (lane 2) indicates that the strain was not fully segregated. The heterozygous mutant strain CSR27 was sensitive to SDS, proteinase K, and to some extent lysozyme (weak growth in the presence of 30 μg lysozyme/ml [Fig. 4C]), indicating the presence of an envelope with altered permeability. The sensitivity to SDS may imply that outer membrane integrity is affected by an altered PG, but lack of (or low) sensitivity to erythromycin indicates less alteration than in mutants directly affecting outer membrane formation (33). The sensitivity to proteinase K and lysozyme may indicate, on the other hand, the presence of a weak PG because of D-alanine scarcity. Remarkably, whereas CSR27 was sensitive to proteinase K and lysozyme, AFS-I-*sjcF1* was not (Fig. 4C). Quantification of labeling with Van-FL yielded a decrease in vancomycin incorporation, as judged from values for filament ends, cell sides, and cell-cell contact sites in the mutant compared to the wild type ($P <$ 0.005) (Fig. 4D). The distinct phenotype of CSR27 supports that Alr2458 but not SjcF1 is involved generally in PG biogenesis.

The SjcF1 protein is involved in restriction of the peptidoglycan channel. The distribution of SjcF1 in cells was analyzed with antibodies recognizing the protein followed by immunofluorescence (Fig. 5A and B). The specificity of the antibody was confirmed by immunodecoration of cell lysates and overexpressed protein (Fig. 5C). Despite lack of complete mutant chromosome segregation, no significant content of the protein was found in strain AFS-I-*sjcF1*, whereas the protein was detectable in the outer rim of wild-type cells. By visual inspection (Fig. 5A) and quantification of the fluorescence of the individual PG layer even in the
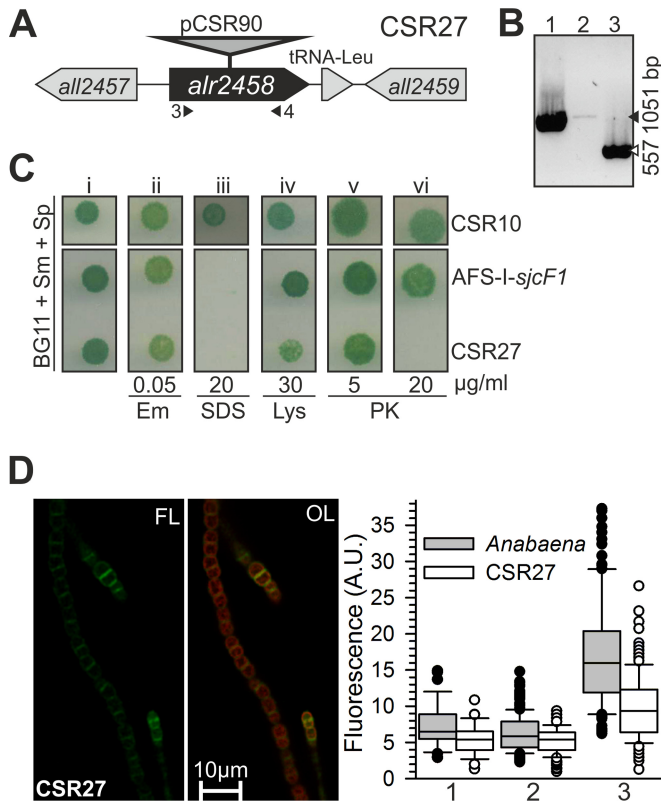
FIG 4 CSR27 is a mutant of an alanine racemase influencing peptidoglycan functionality. (A) Schematic representation of the *alr2458* locus with indication of plasmid insertion (strain CSR27). Triangles indicate the positions of primers used for strain analysis. (B) PCR analysis of the genetic structure of the *alr2458* region in *Anabaena* (lane 1) and in CSR27 (lane 2) with *alr2458* primers, as well as in CSR27 with *alr2355* primers used as a positive control for the presence of DNA (lane 3). Black triangle, 1,051 bp; white triangle, 557 bp. (C) Strains CSR10 and AFS-I-*sjcF1* were grown on BG11 plates with Sp/Sm (i) containing 50 ng/ml erythromycin (Em [ii]), 20 µg/ml SDS (iii), 30 µg/ml lysozyme (Lys [iv]), or 5 (v) and 20 (vi) µg/ml proteinase K (PK) and photographed after 8 days of incubation. (D) CSR27 filaments grown in BG11 were incubated with Van-FL and analyzed by CLSM. Controls are shown in Fig. S2 in the supplemental material. Shown is Van-FL fluorescence (FL) and the overlay with autofluorescence (OL). The quantification of individual cells (≥15 different filaments) of CSR27 (white) is shown; for comparison, *Anabaena* (gray) is reproduced from Fig. 3D. A.U., arbitrary units.

septum (Fig. 5B), we observed a significantly higher intensity in the septal region than the other cell wall sections. On average, the level in the septal PG of a cell was about 2.1-fold higher than the level in lateral cell walls (Fig. 5B). Thus, septal regions had about 4-fold-higher levels of SjcF1 than lateral walls.

SjcF1 physically interacts with PG (Fig. 1) and is significantly localized in the septal region. Hence, the structure of the PG isolated from AFS-I-*sjcF1*, CSR27, and *Anabaena* was analyzed by electron microscopy. Whereas we did not find evidence for an altered structure in the overall sacculus of AFS-I-*sjcF1*, we realized an altered morphology of the channels (also known as nanopores) found in high-density PG regions thought to be caused by juxtaposition (likely involving chemical interaction) of the PG layers from adjacent cells (23). These perforations (nanopores) may correspond to the channels through which the septal junction complexes traverse the PG layer (7, 23). In strain CSR27 (Fig. 5E) and the wild type (Fig. 5F), the diameter of the channels is rather

restricted: on average, 21 nm (sigma from Gaussian distribution, 2.1 nm [Fig. 5G]) and 19 nm (sigma, 3.5 nm), respectively. For AFS-I-*sjcF1* already visual inspection revealed a broad distribution of septal junction channel sizes (Fig. 5D). Quantification yielded a significantly different diameter of 29 nm with a very broad distribution (sigma, 8.2 nm; one-way analysis of variance [ANOVA] test) (see Table S2 in the supplemental material).

SjcF1 is functionally linked to the septal junction complexes. Intercellular molecular exchange in *Anabaena* and the AFS-I-*sjcF1* mutant was investigated as transfer of fluorescent calcein analyzed by fluorescence recovery after photobleaching (FRAP) (14) (Fig. 6A). Calcein has a diffusion constant of $D = 1.5 \times 10^{-6}\,\mathrm{cm^2/s}$ in solution and in endosomes (35, 36). Assuming free diffusion, a recovery time of 0.1 to 0.3 s is expected (see Fig. S3 in the supplemental material). Consistent with previous reports (14, 21), the membrane provides a resistance for full recovery of fluorescence (Fig. 6B). The estimated exchange coefficient (ec) for the *Anabaena* wild type was $ec_{wt} = 0.033 \pm 0.005\,\mathrm{s^{-1}}$ ($n = 27$), similar to that described previously (14). For the AFS-I-*sjcF1* mutant, we observed a reduced recovery rate, $ec_{MT} = 0.011 \pm 0.003\,\mathrm{s^{-1}}$ ($n = 37$), and the difference is significant with $P < 0.001$ (t test). The 3-fold reduction is comparable to the defect observed for a $\Delta fraG$ ($\Delta sepJ$) strain (14) and links the function of SjcF1 to that of septal junction complexes allowing the transfer of calcein between cells.

SepJ, FraC, and FraD (14, 19–22) are possible components of septal junction complexes, which most likely traverse the septal junction channels. An analysis of the transcripts from the coding genes for the three factors in AFS-I-*sjcF1* showed a significant increase of abundance compared to the wild type (Table 2). In turn, the transcript of *sjcF1* was significantly increased in a mutant of *sepJ* and a triple mutant of *sepJ*, *fraC*, and *fraD* (Table 2). These observations point toward a functional relationship between septal junction complexes and SjcF1.

Moreover, utilizing the program SH3-Hunter (37), SH3 binding motifs can be found in FraC (amino acids [aa] 66 to 72 [FVEPVLP]) and SepJ (aa 326 to 331 [PLTPEK]), but not in FraD or AmiC2 (Fig. 6C). We synthesized fluorescent peptides corresponding to the SH3-binding motifs of FraC (FVEPVLPVP) and SepJ (PLTPEKPPEP) and analyzed their interaction with His-tagged SjcF1 by fluorescence anisotropy. We observed a dissociation constant of $12 \pm 1\,\mu M$ for the interaction between SjcF1 and FraC peptide (Fig. 6D). The interaction between SjcF1 and SepJ peptide was certainly of lower affinity, with a dissociation constant of $39 \pm 3\,\mu M$ (see Fig. S4 in the supplemental material). However, an interaction with a SepJ peptide bearing proline-to-serine substitutions (PLTSEKSSEP) was not observed (Fig. 6D), confirming that interaction with the native peptide was significant.

To confirm complex formation in a more *in vivo*-like situation, we analyzed the interaction between SjcF1 and SepJ, FraC, or FraD by the bacterial two-hybrid system (38). The T18 or T25 complementary fragment of the catalytic subunit of adenylate cyclase was added to the predicted cytoplasmic terminus of SepJ, FraC, SjcF1, or FraD. The β-galactosidase activity was determined in *Escherichia coli* strains carrying the indicated T18 and T25 fusion protein-encoding plasmids (Fig. 6E, white bars). For the control, *E. coli* strains with plasmids producing T18 and/or T25 without fusions were used (black bar). Significant interaction was obtained for SjcF1 and SepJ and for SjcF1 and FraC, but not for SjcF1 and FraD or for SjcF1 with itself. Nonetheless, these interactions are weaker than the very strong SepJ self-interaction (39) used as a
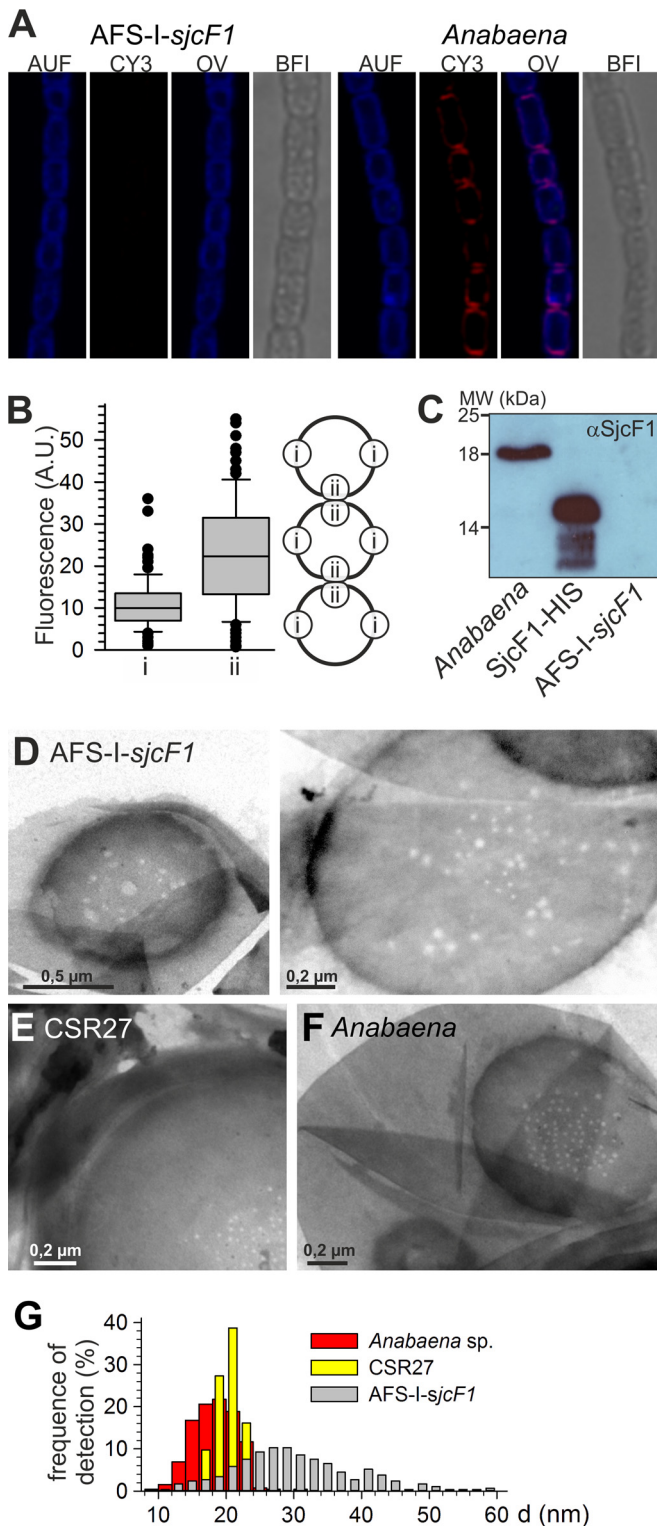
FIG 5 The septal junction channels in the peptidoglycan layer. (A) AFS-I-*sjcF1* (left) or *Anabaena* (right) was incubated with anti-SjcF1-CY3, and cells were analyzed by confocal laser scanning microscopy. Cyanobacterial autofluorescence (AUF), CY3 signal (CY3), the overlay (OL), and the bright-field image (BFI) are shown. (B) CY3-FL fluorescence of individual cells at positions i and ii (see model on the right) of cells of 5 different filaments of *Anabaena* was quantified (*t* test for significance of the difference, *P* < 0.001). In this case, the signals from the two individual cells in the septum can be separated (A) and were analyzed individually. (C) Immunodecoration with SjcF1

(Continued)

positive control (Fig. 6E). This is consistent with the low affinity determined by fluorescence anisotropy measurements and the presence of the SH3 binding module in the periplasm, which might not induce a tight interaction between the membrane helices of the interaction partners (Fig. 6C).

DISCUSSION

It is generally accepted that cells in an *Anabaena* filament exchange regulators and metabolites. Two alternative routes have been considered: one utilizing the periplasm (2, 11) and another utilizing septal junction complexes (2, 14, 21, 22). While components for active transport through the periplasm, which might be required due to its gel-like texture (12), have not been described, the FraC, FraD, and SepJ proteins have been identified as putative components of the septal junction complexes (e.g., see references 14, 21, and 22). Based on functional analysis (i.e., transfer of fluorescent tracers and a fluorescent sucrose analog), these proteins may be part of two different types of complexes, one containing SepJ and another containing FraC and FraD (22, 40). However, only one type of septal junction has been noted structurally, with an outer diameter of about 15 to 20 nm (15–18) and an inner diameter of about 6 nm (7). For formation of the septal junctions, a channel has to span the 24-nm-thick septal PG layer (7). Recently, proteins of the AmiC family of amidases have been discussed to function in the formation of such channels or "nanopores" (23, 24).

We isolated *Anabaena* mutants of an alanine racemase (Alr2458) and of SjcF1 (All1861). Although mutant chromosomes could not be segregated, heterozygous mutants could be maintained and investigated, because *Anabaena* is known to be polyploid (41). In strain AFS-I-*sjcF1*, the *sjcF1* gene dosage seems indeed to be too low to produce detectable levels of the protein SjcF1 (Fig. 5A to C). The low gene dosages led to alterations of the phenotypes of both strains (for instance, sensitivity to SDS), indicating that they bear an altered cell envelope. However, the *alr2458* mutant is affected in PG synthesis and stability, as judged by (i) lower incorporation of vancomycin than in the wild type and (ii) sensitivity to proteinase K and lysozyme, which is not observed and not as drastic as for AFS-I-*sjcF1*, respectively (Fig. 3 and 4). Thus, the alanine racemase appears to be directly involved in PG synthesis, while SjcF1 is not.

SjcF1 was previously identified in cell wall preparations of both vegetative cells and heterocysts (25, 26). We observed a temporary downregulation of *sjcF1* expression during early heterocyst formation induced by nitrogen depletion (Fig. 2) and an upregulation in response to enhanced metal levels (Fig. 2). Metals are known to bind to PG (30, 31) and thus, the observed metal regulation of expression might indicate a relationship of SjcF1 with general PG function. Additionally, it has been reported that *sjcF1*

Figure Legend Continued

antibodies of cell extracts (1 μg protein) from *Anabaena* and AFS-I-*sjcF1* and of recombinant His-tagged SjcF1 without the 2nd PG binding domain. (D to F) Sacculi from AFS-I-*sjcF1* (D [two micrographs shown]), CSR27 (E), and *Anabaena* (F) grown in BG11 medium were isolated and visualized by electron microscopy. Representative images are shown. (G) Quantitative analysis of channel dimensions from at least two biological independent replicas is presented for 524 septal junction channels of *Anabaena*, 581 of ASF-I-*sjcF1*, and 93 of CSR27. Results were binned in 2-nm steps, and the percentage of each bin is shown. Statistical values are given in Table S2 in the supplemental material.
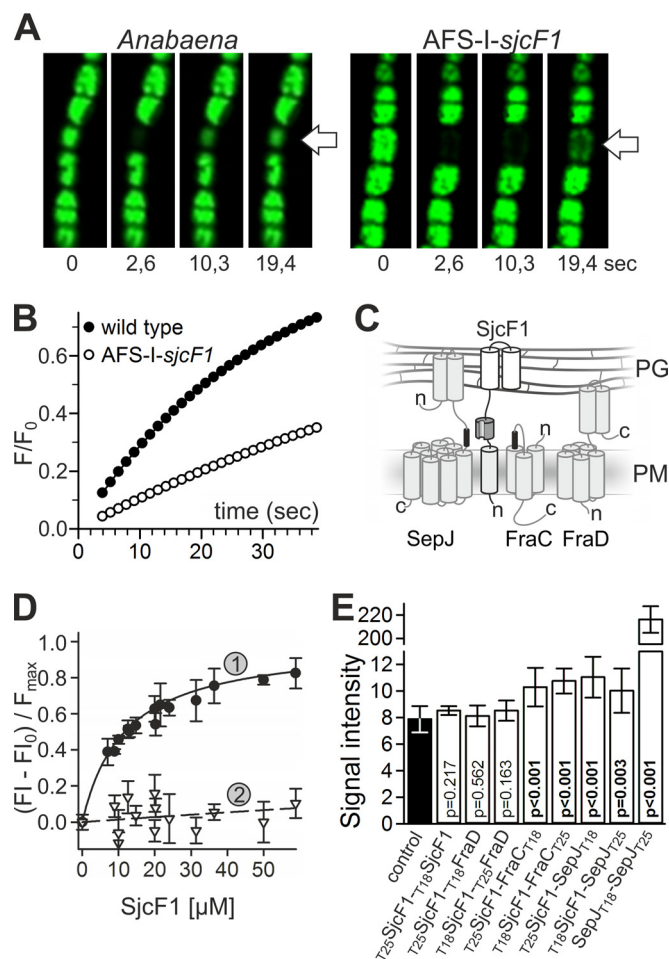
FIG 6 Relation of SjcF1 to septal junction complexes. (A) Representative time series of calcein recovery in the *Anabaena* wild-type and AFS-I-*sjcF1* strains. The first image is before the bleach pulse; the times after the bleaching are indicated. (B) Recovery rate of calcein fluorescence for a representative measurement in the *Anabaena* wild-type and AFS-I-*sjcF1* strains. (C) Scheme of the topology of SepJ, FraC, FraD, and SjcF1 (see the material in the expanded view) in the plasma membrane (PM) and the periplasm (PG, peptidoglycan). Transmembrane domains in the PM, the coiled-coil domains of SepJ and FraD in the periplasm (grey cylinders), the PG binding domains of SjcF1 (white cylinders), the SH3 domain (dark gray), and the SH3 binding motifs (black) are indicated. (D) Fluorescent-labeled peptide representing the SH3 binding motif of FraC (1, FVEPVLPVPI; K_D, 12 ± 1 μM) or a mutated version of the SepJ motif (2, PLTSEKSSEP; K_D, >2 mM) was incubated with increasing concentrations of His-tagged SjcF1. The fluorescent anisotropy was analyzed. For representation, the initial value was subtracted and the curve was normalized to the maximal expected value. The lines indicate the least square fit analysis to the equation $F = F_{max} \times [SjcF1]/(K_D + [SjcF1])$. (E) The average of the β-galactosidase activity of *E. coli* with plasmid combinations producing the indicated proteins (white bars) and of the controls of either two empty plasmids (producing T18 and T25) or one empty and one fusion protein-encoding plasmid in all combinations possible (black bar) is shown with the standard deviation. Probability values of the *t* test for significance of the differences are indicated (p).

is induced after 3 days of iron starvation with a subsequent decline after 7 days (42), which might suggest a restructuring of PG in response to oxidizing conditions.

The *sjcF1* mutant specifically deviates in the size of septal junction channels. Consistent with a specific role of SjcF1, the alanine racemase mutation has only a small effect on channel formation

(Fig. 5). Moreover, the intercellular transfer of calcein in the *sjcF1* mutant (Fig. 6) is affected in a similar manner as in the *sepJ* mutant (14). This is consistent with the broad distribution of the septal junction channel diameter in the *sjcF1* insertional mutant (Fig. 5), which might hint at a malfunction of the septal junction protein complex leading to reduced metabolite exchange. Thus, whereas the previously described AmiC proteins are amidases likely involved in channel formation (8, 23), SjcF1 function appears to be related to it, resulting in restriction of the diameter of the channel (Fig. 5).

Next to the studies on the *sjcF1* mutant, the analysis of the protein function further supports a link between SjcF1 function and septal junction channel distribution. SjcF1 contains two functional PG-binding domains (Fig. 1) that most likely ensure anchoring of the protein to the PG. Consistently SjcF1 is localized to the cell walls and the intercellular septa (Fig. 5). However, SjcF1 does not contain a domain accounting for an enzymatic activity and thus is probably not involved in PG layer synthesis *per se* (Fig. 1 and 3), but it contains an SH3 domain for protein-protein interactions (Fig. 1) (27). Proteins with the same architecture as SjcF1 are only found in filamentous cyanobacteria (Fig. 1). In line with a relationship between septal junction channel function and SjcF1 activity, SjcF1 recognizes the SH3-binding motifs of FraC and SepJ and interacts with both proteins in a bacterial two-hybrid analysis (Fig. 6). Moreover, while being localized in the outer rim of the entire cell, SjcF1 is enriched in the intercellular septa (Fig. 5) where the septal proteins SepJ, FraC, and FraD are localized (19, 21, 22). In addition, *fraC*, *fraD*, and *sepJ* are upregulated in AFS-I-*sjcF1*, and expression of *sjcF1* is significantly enhanced in a *sepJ* mutant and a mutant with mutation of all of these septal factors (Table 2). This is consistent with the observed alteration of the septal junction channel diameter in the *sjcF1* insertional mutant (Fig. 5). However, perhaps because of the presence of septal junction channels, albeit with altered diameter, strain AFS-I-*sjcF1* does not show a fragmentation phenotype (43), which is characteristic for the mutants of some proteins directly involved in septal junction complex formation (5, 19–21).

Considering the presented results, it can be suggested that SjcF1 interacts with FraC and SepJ to arrange the septal junction complexes in the PG layer. Thereby, SjcF1 would bridge the septal junction complexes to the PG layer. The absence of such a bridge apparently disturbs the refinement of channel dimension in the septal PG but not its existence. In turn, the disturbance of the channel dimension has a negative effect on the efficiency of molecular transfer through the septal junction complex as judged from the decreased rate of intercellular calcein transfer (Fig. 6). Thus, the identification of SjcF1 expands our understanding of septal junction formation. Possible components of the septal junction complexes themselves, namely, SepJ, FraC, and FraD, and at least two components securing that septal junction complexes traverse the septal PG layer, namely, an AmiC amidase and SjcF1, have now been identified. Whereas AmiC appears to be involved in the formation of perforations in the septal PG, SjcF1 influences their dimension and may bridge the septal junction complexes with the PG layer. Nonetheless, based on the localization of SjcF1 in the entire outer rim of the cell, FraC and SepJ might not be the only interaction partners of SjcF1. Consistently with this idea, 270 proteins predicted to be secreted out of the cytoplasm and bearing an SH3 target motif (PXXPX[RK] or [RKHYFW]XXPXXP) in a soluble domain are encoded in the

TABLE 2 Transcript abundance of genes involved in septal junction complex formation[a]

Strain	sepJ		fraC		fraD		sjcF1	
	$\Delta\Delta G$[b]	Fold[c]	$\Delta\Delta G$[b]	Fold[c]	$\Delta\Delta G$[b]	Fold[c]	$\Delta\Delta G$[b]	Fold[c]
CSVM34 ($\Delta sepJ$)	4 ± 1	0.05[d]	−1.2 ± 0.5	**2.3**[e]	**−4.3 ± 0.3**	**20**[f]	**−2.3 ± 0.1**	**5.1**[f]
CSVT1 ($\Delta fraC$)	**−2.3 ± 0.5**	**5.0**[f]	4 ± 1	0.05[d]	**−2.8 ± 0.2**	**6.8**[f]	−0.37 ± 0.02	1.3
CSVM141 ($\Delta sepJ$ $\Delta fraC$ $\Delta fraD$)	4 ± 1	0.05[d]	4 ± 1	0.05[d]	5.4 ± 0.3	0.03[d]	**−1.8 ± 0.1**	**3.5**[f]
AFS-I-sjcF1	−1.3 ± 0.5	**2.5**[e]	**−2.2 ± 0.5**	**4.8**[f]	**−3.4 ± 0.3**	**11**[f]	3.2 ± 0.2	0.1[d]

[a] The transcript abundance for genes encoding septal junction complex proteins and SjcF1 was analyzed by qRT-PCR in BG11-grown cells of the indicated mutant strains. Bold highlights the values with significant changes in comparison to wild type.
[b] Normalized to expression of *rnpB*.
[c] Fold change in mutant.
[d] Background.
[e] Significant at P < 0.005.
[f] Significant at P < 0.001.

Anabaena genome (see Table S6 in the supplemental material). Considering that our results strongly suggest that SjcF1 is not involved in PG synthesis, while the *sjcF1* mutant is sensitive to SDS, SjcF1 might be required for connection of outer and inner membrane proteins to the PG layer for stabilization rather than for recruitment of PG-modifying enzymes to the PG. Nevertheless, possible functions of SjcF1 besides the regulation of septal junction complex formation need to be explored in the future.

MATERIALS AND METHODS

Bioinformatic approaches. For the identification of bacterial proteins containing the Pfam (44) domains SH3_3 (PF08239) and PG_binding_1 (PF01471), regardless of the domain order, we searched in the nr database (45) using HMMER (46). These sequences were screened for additional Pfam domains using the PfamScan script (see Table S1 in the supplemental material).

Recombinant protein expression. To generate SjcF1 fused to an N-terminal His tag for recombinant protein expression, full-length sequence of *sjcF1* (*all1861*) was obtained from Cyanobase (47), and TM domains were predicted as described in the supplemental material. The coding sequence of *all1861* without transmembrane domain (bp 193 to 810 [see Table S5 in the supplemental material]) was amplified by PCR on genomic DNA of *Anabaena* using oligonucleotides containing BamHI and HindIII restriction sites (see Table S3 in the supplemental material). The SjcF1$_{\Delta PG2}$ and SjcF1$_{PG2}$ constructs for recombinant protein expression were produced by amplification of the coding sequence of the SH3 and PG binding domain 1 (bp 193 to 594) and the PG binding domain 2 (bp 601 to 810), respectively. Restricted PCR products were cloned into pQEA8 (Amp^r) see Table S4 in the supplemental material) downstream of the 6× histidine tag coding region. Constructs were verified by sequencing (GATC Biotech AG, Constance, Germany). Proteins were expressed in *E. coli* BL21star/pRosetta/pRep4 (Km^r Cm^r) in 2 liters LB medium for 3 h at 37°C. Cells were harvested by centrifugation (5,000 rpm, 4°C, 10 min), resuspended with a mixture of 50 mM Tris (pH 7.5), 150 mM NaCl, 1 mM MgCl$_2$, and 1 mM phenylmethylsulfonyl fluoride (PMSF), and lysed by passing through a French pressure cell at 20,000 lb/in². After low-speed centrifugation to remove the cell debris, the supernatant was incubated with Ni-nitrilotriacetic acid (NTA) resin (Qiagen, Hilden, Germany), washed 4 times with a mixture of 50 mM Tris (pH 7.5), 150 mM NaCl, 1 mM MgCl$_2$, and 40 mM imidazole, and eluted in the same buffer with 500 mM imidazole.

Peptidoglycan layer binding. Isolation of PG from *Anabaena* and transmission electron microscopy were performed as described in reference 8, using trypsin instead of α-chymotrypsin. The *in vitro* PG binding assay was adapted from reference 48. In brief, 50 μg of purified protein was centrifuged for 15 min at 4°C and 300,000 × *g*. The pellet was collected for analysis. The supernatant was mixed with 50 μl isolated PG layer and incubated for 20 min at room temperature. The mixture was centri-

fuged for 15 min at 4°C and 300,000 × *g*, the supernatant was collected for analysis, and the pellet was washed with 10 mM sodium phosphate (pH 6.8) and 500 mM NaCl. After centrifugation, the pellet and supernatant fractions were supplemented with Laemmli buffer up to uniform volume. To control for protein precipitation, the same procedure was done without addition of the PG layer. All samples were analyzed by Western blotting with an anti-His tag antibody (GE Healthcare, Munich, Germany). Transmission electron microscopy was performed using a Philips CM12 microscope.

Anabaena strain construction and growth. Mutants were generated by previously described methods (49–52) using standard plasmids (49, 50, 53) (see Table S4 in the supplemental material). To generate mutant strain AFS-I-sjcF1, an internal fragment of *sjcF1* was amplified by PCR on *Anabaena* genomic DNA using oligonucleotides containing BamHI restriction sites (see Table S3 in the supplemental material). The restricted PCR product was cloned into pCSV3 (see Table S4). To generate GFP promoter fusion strain AFS-PDGF-*sjcF1*, 740 bp of the region upstream of *sjcF1* including the first 30 bp of the coding region was amplified by PCR on *Anabaena* genomic DNA using oligonucleotides containing BstBI/EcoRV restriction sites. Restricted PCR products were further cloned into pCSEL21 upstream of the *gfp* open reading frame (ORF). Fusion fragments were excised by digestion with PstI/EcoRI and ligated into cargo vector pCSEL24 for homologous recombination (50). Conjugation into *Anabaena* was done as described previously (51, 54). The mutant strain AFS-I-P24 is a *nucA-nuiA* (*all7361-all7362*) single recombinant mutant of *Anabaena* generated by integration of plasmid pCSEL24 into the *nucA-nuiA* region (51, 54, 55).

To inactivate the alanine racemase gene, an internal 449-bp fragment of *alr2458* was amplified by PCR using primers alr2458-1 and alr2458-2 (with BamHI restriction sites at the 5′ ends [461 bp]) and *Anabaena* genomic DNA. The amplified fragment was cloned into vector pMBL-T (Dominion MBL), producing pCSR82, and transferred as a BamHI-ended fragment to BamHI-digested pCSV3, producing pCSR90 (Sm^r Sp^r). Conjugation of *Anabaena* with *E. coli* HB101 carrying pCSR90 with helper and methylation plasmid pRL623 was effected by the conjugative plasmid pRL443, carried in *E. coli* ED8654, and performed with selection for resistance to Sm and Sp. The genomic structure of selected clones was studied by PCR on isolated DNA with the primer pair alr2458-3 and alr2458-4 yielding 1,051 bp (wild type) or ~5.5 kb (mutant). The insertion mutant, which was checked to contain the new genomic structure in *alr2458*, although it could not be segregated, was designated strain CSR27.

Growth of *Anabaena* strains (21, 22, 33, 51, 52) (Table 1) and preparation of plates were done as described previously (54). Cells were spotted on BG11 agar medium in the presence or absence of the indicated concentrations of antibiotics, lysozyme, SDS, and proteinase K. Physiological parameters were determined as described previously (56, 57). In brief, pulse amplitude modulation (PAM) analysis of chlorophyll *a* fluorescence of *Anabaena* strains using a mini-imaging PAM chlorophyll fluorimeter (Heinz Walz GmbH, Effeltrich, Germany) was performed as described

previously (56). The effective PSII quantum yield, $\Phi(II)$, and the electron transport rate (ETR) were calculated as described previously (57). Lipid extraction and analysis were done as described previously (51).

DNA and RNA isolation and analysis. RNA and DNA isolation, segregation analysis, RT-PCR, and quantitative RT-PCR (qRT-PCR) analysis were performed by standard procedures (58). The oligodeoxynucleotides used are listed in Table S3 in the supplemental material. Southern blotting was performed by standard procedures (59) using ^{32}P-labeled DNA as a probe produced by PCR and radioactively labeled by use of Ready-to-Go DNA labeling beads from GE Healthcare (Munich, Germany). Genomic DNA was digested with HindIII.

Fluorescence analysis. GFP fluorescence of AFS-PDGF-*sjcF1* was visualized as described previously (51). The methods for preparation of the Van–FL stain and staining of *Anabaena* were adapted from reference 34. In brief, *Anabaena* cells were diluted to an optical density at 750 nm (OD_{750}) of 0.6 and on the next day incubated with 2 μg/ml of Van-FL for 1 h in the dark. Before visualization, cells were washed two times with BG11 medium. For the negative control, cells were incubated with the same concentration of uncoupled vancomycin. Fluorescence microscopy was performed using a Leica SP5 confocal laser scanning microscope with an HCX PL APO CS 40¥ 1.25 NA oil objective. Van-FL was excited at 488 nm, and fluorescence was monitored in the range from 500 to 520 nm. Chlorophyll *a* autofluorescence was detected through a window from 630 to 700 nm.

Immunofluorescence analysis. Immunofluorescence was performed as described previously (60). In brief, 1 ml of *Anabaena* culture in BG11 was pelleted and fixed in a mixture of 100 mM PIPES [piperazine-*N,N'*-bis(2-ethanesulfonic acid)], 1 mM $MgSO_4$, and 2 mM EGTA (pH 6.9) (MtSB buffer) containing 3.7% paraformaldehyde. After being washed twice with MtSB, cells were permeabilized with 0.5% Triton X-100 for 15 min and 0.1 M Tris-HCl (pH 8.0) for 15 min. After being pelleted and resuspended in 100 μl phosphate-buffered saline (PBS), cells were spotted on coverslips coated with poly-L-lysine. Coverslips were washed twice in PBS for 5 min and blocked using 0.1 M glycine in PBS for 15 min and 1% bovine serum albumin (BSA) in PBS for 30 min. Coverslips were incubated with anti-SjcF1 peptide antibodies (PSL GmbH) in 1% BSA–PBS overnight at 4°C. After being washed twice in PBS, coverslips were incubated with secondary fluorochrome-labeled antiserum (rabbit anti-Cy3; Sigma-Aldrich) in 1% BSA–PBS for 1.5 h at room temperature. Fluorescence was recorded using the Leica SP5 (excitation at 561 nm; emission between 564 and 620 nm). Cyanobacterial autofluorescence was recorded between 640 and 750 nm.

FRAP analysis. FRAP measurements and labeling of *Anabaena* with calcein-AM (Sigma-Aldrich) was performed as described previously (14). In brief, after incubation with calcein and washing with BG11, 5 μl cells was mixed with 50 μl BG11 medium containing 1% low-melting-temperature agar and spotted on an object slide. FRAP measurements were performed using the Leica SP5 with the program Leica Microsystems, Las AF, FRAP Wizard (excitation with argon laser [488 nm] with 15% power, emission at 500 to 527 nm with smart gain of 562 nm and pinhole of 95 μm, 63× oil-immersion objective, and zoom factor of 2.5). For bleaching, the "zoom in" approach was chosen, and the laser power increased to 23%. All other parameters were kept constant. The bleaching area was adjusted to the size of a single cell. The bleaching length and interval between single images were set to 1.2 s. Before bleaching, 2 images were taken, and recovery of the fluorescence signal was recorded for 40 s. The intensity of the fluorescence signal was quantified using ImageJ, and the data were processed with SigmaPlot 12.

Anisotropy measurements. Two hundred micromoles of peptide was labeled with 2 μM *N*-(5-fluorescenyl)-maleimide (Sigma-Aldrich) in a mixture of 50 mM HEPES (pH 7.0), 150 mM NaCl, and 5 mM $MgCl_2$. The protein concentration of His-tagged SjcF1 in elution buffer (50 mM HEPES [pH 6.8], 150 mM NaCl, 1 mM $MgCl_2$, 500 mM imidazole) was determined by Bradford spectrometry. Anisotropy (excitation, 492 nm;

emission, 522 nm) was measured by using Fluorolog and a Horiba Jobin Yvok spectrometer with a constant fluorophore concentration of 50 nM.

Bacterial two-hybrid analysis. Constructs were prepared as described previously (39, 61). To construct a T18 or T25 fusion protein, *all1861* was amplified using primers all1861-1 and all1861-2 (see Table S3 in the supplemental material). The amplified fragment was digested with BamHI and KpnI and cloned into the pKT25 vector, producing pCSFR56, which expresses the T25 fusion protein, or into pUT18C, producing pCSFR57, which expresses the T18 fusion protein (61). Construction of the fusions with the whole SepJ protein have been described previously (39) and with FraC and FraD will be described elsewhere (J. E. Frías and E. Flores, unpublished data). Plasmids were cotransformed into BTH101 (*cya-99*). Transformants were plated onto LB medium containing selective antibiotics and 1% glucose. Efficiencies of interactions between different hybrid proteins were quantified by measurement of β-galactosidase activity in cells from liquid cultures.

Bacteria were grown in LB medium in the presence of 0.5 mM isopropyl-β-D-thiogalactopyranoside (IPTG) and appropriate antibiotics at 30°C for 16 h. Before the assays, cultures were diluted 1:5 into buffer Z (60 mM Na_2HPO_4, 40 mM NaH_2PO_4, 10 mM KCl, 1 mM $MgSO_4$). To permeabilize cells, 30 μl of toluene and 35 μl of a 0.1% SDS solution were added to 2.5 ml of bacterial suspension. The tubes were vortexed for 10 s and incubated with agitation at 37°C for 45 min for evaporation of toluene. For the enzymatic reaction, 875 μl of permeabilized cells was added to buffer Z supplemented with β-mercaptoethanol (25 mM final concentration), to a final volume of 3.375 ml. The tubes were incubated at 30°C in a water bath for at least 5 min. The reaction was started by adding 875 μl of 0.4 mg·ml^{-1} *o*-nitrophenol-β-galactoside (ONPG) in buffer Z. One-milliliter samples taken at different times (up to 10 min) were added to 0.5 ml of 1 M Na_2CO_3 to stop the reaction. The A_{420} was recorded, and the amount of *o*-nitrophenol produced was calculated using an extinction coefficient of $\varepsilon_{420} = 4.5$ mM^{-1} cm^{-1} and referred to the amount of total protein, determined by a modified Lowry procedure. The *o*-nitrophenol produced per milligram of protein versus time was represented, and β-galactosidase activity was deduced from the slope of the linear function. The activity in Fig. 6E (signal intensity) corresponds to nanomoles of *o*-nitrophenol (per milligram of protein) per minute.

Transmembrane domain prediction. Different prediction programs were used to define a consensus for the number of transmembrane helices (helical TM) for FraC (3 helical TM [see Table S5 in the supplemental material]), FraD (5 TM [see Table S5]), SjcF1 (1 TM [see Table S5]), and SepJ (9 TM [see Table S5]). The programs used are DAS (62), MEMSAT (63), TM-Pred (64), SOSUI (65), SPLIT (66), Minnou (67), TM-Finder (68), TopCon (69), PHDhtm (70), and TMHMM (71).

SUPPLEMENTAL MATERIAL

Supplemental material for this article may be found at http://mbio.asm.org/lookup/suppl/doi:10.1128/mBio.00376-15/-/DCSupplemental.

Figure S1, PDF file, 0.3 MB.
Figure S2, PDF file, 0.2 MB.
Figure S3, PDF file, 0.3 MB.
Figure S4, PDF file, 0.2 MB.
Table S1, PDF file, 0.1 MB.
Table S2, PDF file, 0.02 MB.
Table S3, PDF file, 0.02 MB.
Table S4, PDF file, 0.1 MB.
Table S5, PDF file, 0.03 MB.
Table S6, PDF file, 0.04 MB.

ACKNOWLEDGMENTS

REFERENCES

1. **Flores E, Herrero A.** 2010. Compartmentalized function through cell differentiation in filamentous cyanobacteria. Nat Rev Microbiol **8:**39–50. http://dx.doi.org/10.1038/nrmicro2242.

2. **Flores E, Herrero A, Wolk CP, Maldener I.** 2006. Is the periplasm continuous in filamentous multicellular cyanobacteria? Trends Microbiol **14:**439–443. http://dx.doi.org/10.1016/j.tim.2006.08.007.

3. **Ris H, Singh RN.** 1961. Electron microscope studies on blue-green algae. J Biophys Biochem Cytol **9:**63–80. http://dx.doi.org/10.1083/jcb.9.1.63.

4. **Hoiczyk E, Baumeister W.** 1995. Envelope structure of four gliding filamentous cyanobacteria. J Bacteriol **177:**2387–2395.

5. **Bauer CC, Buikema WJ, Black K, Haselkorn R.** 1995. A short-filament mutant of *Anabaena* sp. strain PCC 7120 that fragments in nitrogen-deficient medium. J Bacteriol **177:**1520–1526.

6. **Schleifer KH, Kandler O.** 1972. Peptidoglycan types of bacterial cell walls and their taxonomic implications. Bacteriol Rev **36:**407–477.

7. **Wilk L, Strauss M, Rudolf M, Nicolaisen K, Flores E, Kühlbrandt W, Schleiff E.** 2011. Outer membrane continuity and septosome formation between vegetative cells in the filaments of *Anabaena* sp. PCC 7120. Cell Microbiol **13:**1744–1754. http://dx.doi.org/10.1111/j.1462-5822.2011.01655.x.

8. **Lehner J, Zhang Y, Berendt S, Rasse TM, Forchhammer K, Maldener I.** 2011. The morphogene AmiC2 is pivotal for multicellular development in the cyanobacterium *Nostoc punctiforme*. Mol Microbiol **79:**1655–1669. http://dx.doi.org/10.1111/j.1365-2958.2011.07554.x.

9. **Hahn A, Schleiff E.** 2014. The cell envelope, p 29–88. *In* The cell biology of cyanobacteria Flores E, Herrero A (ed). Caister Academic Press, Norfolk, United Kingdom.

10. **Jürgens UJ, Weckesser J.** 1986. Polysaccharide covalently linked to the peptidoglycan of the cyanobacterium *Synechocystis* sp. strain PCC6714. J Bacteriol **168:**568–573.

11. **Mariscal V, Herrero A, Flores E.** 2007. Continuous periplasm in a filamentous, heterocyst-forming cyanobacterium. Mol Microbiol **65:**1139–1145. http://dx.doi.org/10.1111/j.1365-2958.2007.05856.x.

12. **Hobot JA, Carlemalm E, Villiger W, Kellenberger E.** 1984. Periplasmic gel: new concept resulting from the reinvestigation of bacterial cell envelope ultrastructure by new methods. J Bacteriol **160:**143–152.

13. **Zhang LC, Chen YF, Chen WL, Zhang CC.** 2008. Existence of periplasmic barriers preventing green fluorescent protein diffusion from cell to cell in the cyanobacterium *Anabaena* sp. strain PCC 7120. Mol Microbiol **70:**814–823. http://dx.doi.org/10.1111/j.1365-2958.2008.06476.x.

14. **Mullineaux CW, Mariscal V, Nenninger A, Khanum H, Herrero A, Flores E, Adams DG.** 2008. Mechanism of intercellular molecular exchange in heterocystforming cyanobacteria. EMBO J **27:**1299–1308. http://dx.doi.org/10.1038/emboj.2008.66.

15. **Pankratz HS, Bowen CC.** 1963. Cytology of blue-green algae. I. The cells of *Symploca muscorum*. Am J Bot **50:**387–399.

16. **Wildon DC, Mercer FV.** 1963. The ultrastructure of the heterocyst and akinete of the blue-green algae. Arch Microbiol **47:**19–31. http://dx.doi.org/10.1007/BF00408286.

17. **Giddings TH, Jr, Staehelin LA.** 1981. Observation of microplasmodesmata in both heterocyst-forming and non-heterocyst forming filamentous cyanobacteria by freeze-fracture electron microscopy. Arch Microbiol **129:**295–298. http://dx.doi.org/10.1007/BF00414700.

18. **Omairi-Nasser A, Haselkorn R, Austin J III.** 2014. Visualization of channels connecting cells in filamentous nitrogen-fixing cyanobacteria. FASEB J **28:**3016–3022. http://dx.doi.org/10.1096/fj.14-252007.

19. **Flores E, Pernil R, Muro-Pastor AM, Mariscal V, Maldener I, Lechno-Yossef S, Fan Q, Wolk CP, Herrero A.** 2007. Septum-localized protein required for filament integrity and diazotrophy in the heterocyst-forming cyanobacterium *Anabaena* sp. strain PCC 7120. J Bacteriol **189:**3884–3890. http://dx.doi.org/10.1128/JB.00085-07.

20. **Nayar AS, Yamaura H, Rajagopalan R, Risser DD, Callahan SM.** 2007. FraG is necessary for filament integrity and heterocyst maturation in the cyanobacterium *Anabaena* sp. strain PCC 7120. Microbiology **153:**601–603. http://dx.doi.org/10.1099/mic.0.2006/002535-0.

21. **Merino-Puerto V, Mariscal V, Mullineaux CW, Herrero A, Flores E.** 2010. Fra proteins influencing filament integrity, diazotrophy and localization of septal protein SepJ in the heterocyst-forming cyanobacterium *Anabaena* sp. Mol Microbiol **75:**1159–1170. http://dx.doi.org/10.1111/j.1365-2958.2009.07031.x.

22. **Merino-Puerto V, Schwarz H, Maldener I, Mariscal V, Mullineaux CW, Herrero A, Flores E.** 2011. FraC/FraD-dependent intercellular molecular exchange in the filaments of a heterocyst-forming cyanobacterium, *Anabaena* sp. Mol Microbiol **82:**87–98. http://dx.doi.org/10.1111/j.1365-2958.2011.07797.x.

23. **Lehner J, Berendt S, Dörsam B, Pérez R, Forchhammer K, Maldener I.** 2013. Prokaryotic multicellularity: a nanopore array for bacterial cell communication. FASEB J **27:**2293–2300. http://dx.doi.org/10.1096/fj.12-225854.

24. **Berendt S, Lehner J, Zhang YV, Rasse TM, Forchhammer K, Maldener I.** 2012. Cell wall amidase AmiC1 is required for cellular communication and heterocyst development in the cyanobacterium *Anabaena* PCC 7120 but not for filament integrity. J Bacteriol **194:**5218–5227. http://dx.doi.org/10.1128/JB.00912-12.

25. **Moslavac S, Bredemeier R, Mirus O, Granvogl B, Eichacker LA, Schleiff E.** 2005. Proteomic analysis of the outer membrane of *Anabaena* sp. strain PCC 7120. J Proteome Res **4:**1330–1338. http://dx.doi.org/10.1021/pr050044c.

26. **Moslavac S, Reisinger V, Berg M, Mirus O, Vosyka O, Plöscher M, Flores E, Eichacker LA, Schleiff E.** 2007. The proteome of the heterocyst cell wall in *Anabaena* sp. PCC 7120. Biol Chem **388:**823–829. http://dx.doi.org/10.1515/BC.2007.079.

27. **Saksela K, Permi P.** 2012. SH3 domain ligand binding: what's the consensus and where's the specificity? FEBS Lett **586:**2609–2614. http://dx.doi.org/10.1016/j.febslet.2012.04.042.

28. **Castillo RM, Mizuguchi K, Dhanaraj V, Albert A, Blundell TL, Murzin AG.** 1999. A six-stranded double-psi beta barrel is shared by several protein superfamilies. Struct Fold Des **7:**227–236. http://dx.doi.org/10.1016/S0969-2126(99)80028-8.

29. **Koenig P, Oreb M, Höfle A, Kaltofen S, Rippe K, Sinning I, Schleiff E, Tews I.** 2008. The GTPase cycle of the chloroplast import receptors Toc33/Toc34: implications from monomeric and dimeric structures. Structure **16:**585–596. http://dx.doi.org/10.1016/j.str.2008.01.008.

30. **Hoyle BD, Beveridge TJ.** 1984. Metal binding by the peptidoglycan sacculus of *Escherichia coli* K-12. Can J Microbiol **30:**204–211. http://dx.doi.org/10.1139/m84-031.

31. **Falla J, Block JC.** 1993. Binding of CD2$^+$, Ni^{2+}, Cu^{2+} and Zn^{2+} by isolated envelopes of *Pseudomonas fluorescens*. FEMS Microbiol Lett **108:**347–352. http://dx.doi.org/10.1111/j.1574-6968.1993.tb06126.x.

32. **Bai W, Zhao K, Asami K.** 2007. Effects of copper on dielectric properties of *E. coli* cells. Colloids Surf B Biointerfaces **58:**105–115. http://dx.doi.org/10.1016/j.colsurfb.2007.02.015.

33. **Nicolaisen K, Mariscal V, Bredemeier R, Pernil R, Moslavac S, López-Igual R, Maldener I, Herrero A, Schleiff E, Flores E.** 2009. The outer membrane of a heterocyst-forming cyanobacterium is a permeability barrier for uptake of metabolites that are exchanged between cells. Mol Microbiol **74:**58–70. http://dx.doi.org/10.1111/j.1365-2958.2009.06850.x.

34. **Daniel RA, Errington J.** 2003. Control of cell morphogenesis in bacteria: two distinct ways to make a rod-shaped cell. Cell **113:**767–776. http://dx.doi.org/10.1016/S0092-8674(03)00421-5.

35. **Brown EB, Wu ES, Zipfel W, Webb WW.** 1999. Measurement of molecular diffusion in solution by multiphoton fluorescence photobleaching recovery. Biophys J **77:**2837–2849. http://dx.doi.org/10.1016/S0006-3495(99)77115-8.

36. **Yoshida N, Tamura M, Kinjo M.** 2000. Fluorescence correlation spectroscopy: a new tool for probing the microenvironment of the internal space of organelles. Single Mol **4:**279–283.

37. **Ferraro E, Peluso D, Via A, Ausiello G, Helmer-Citterich M.** 2007. SH3-Hunter: discovery of SH3 domain interaction sites in proteins. Nucleic Acids Res **35:**W451–W454. http://dx.doi.org/10.1093/nar/gkm296.

38. **Karimova G, Pidoux J, Ullmann A, Ladant D.** 1998. A bacterial two-hybrid system based on a reconstituted signal transduction pathway. Proc Natl Acad Sci U S A **95:**5752–5756. http://dx.doi.org/10.1073/pnas.95.10.5752.

39. **Ramos-León F, Mariscal V, Frías JE, Flores E, Herrero A.** 2015. Divisome-dependent subcellular localization of cell-cell joining protein SepJ in the filamentous cyanobacterium *Anabaena*. Mol Microbiol **96:**566–580. http://dx.doi.org/10.1111/mmi.12956.

40. **Nürnberg DJ, Mariscal V, Bornikoel J, Nieves-Morión M, Krauß N, Herrero A, Maldener I, Flores E, Mullineaux CW.** 2015. Intercellular diffusion of a fluorescent sucrose analog via the septal junctions in a fila-

mentous cyanobacterium. mBio **6**(2):e02109. http://dx.doi.org/10.1128/mBio.02109-14.

41. **Hu B, Yang G, Zhao W, Zhang Y, Zhao J**. 2007. MreB is important for cell shape but not for chromosome segregation of the filamentous cyanobacterium *Anabaena* sp. PCC 7120. Mol Microbiol **63**:1640–1652. http://dx.doi.org/10.1111/j.1365-2958.2007.05618.x.

42. **Narayan OP, Kumari N, Rai LC**. 2011. Iron starvation-induced proteomic changes in *Anabaena* (*Nostoc*) sp. PCC 7120: exploring survival strategy. J Microbiol Biotechnol **21**:136–146. http://dx.doi.org/10.4014/jmb.1009.09021.

43. **Burnat M, Schleiff E, Flores E**. 2014. Cell envelope components influencing filament length in the heterocyst-forming cyanobacterium *Anabaena* sp. strain PCC 7120. J Bacteriol **196**:4026–4035. http://dx.doi.org/10.1128/JB.02128-14.

44. **Punta M, Coggill PC, Eberhardt RY, Mistry J, Tate J, Boursnell C, Pang N, Forslund K, Ceric G, Clements J, Heger A, Holm L, Sonnhammer EL, Eddy SR, Bateman A, Finn RD**. 2012. The Pfam protein families database. Nucleic Acids Res **40**:D290–D301. http://dx.doi.org/10.1093/nar/gkr1065.

45. **Sayers EW, Barrett T, Benson DA, Bolton E, Bryant SH, Canese K, Chetvernin V, Church DM, Dicuccio M, Federhen S, Feolo M, Fingerman IM, Geer LY, Helmberg W, Kapustin Y, Krasnov S, Landsman D, Lipman DJ, Lu Z, Madden TL**. 2012. Database resources of the National Center for Biotechnology Information. Nucleic Acids Res **40**:D13–D25. http://dx.doi.org/10.1093/nar/gkr1184.

46. **Eddy SR**. 2011. Accelerated profile HMM searches. PLOS Comput Biol **7**:e1002195. http://dx.doi.org/10.1371/journal.pcbi.1002195.

47. **Fujisawa T, Okamoto S, Katayama T, Nakao M, Yoshimura H, Kajiya-Kanegae H, Yamamoto S, Yano C, Yanaka Y, Maita H, Kaneko T, Tabata S, Nakamura Y**. 2014. CyanoBase and RhizoBase: databases of manually curated annotations for cyanobacterial and rhizobial genomes. Nucleic Acids Res **42**:D666–D670. http://dx.doi.org/10.1093/nar/gkt1145.

48. **Bouveret E, Bénédetti H, Rigal A, Loret E, Lazdunski C**. 1999. In vitro characterization of peptidoglycan-associated lipoprotein (PAL)-peptidoglycan and PAL-TolB interactions. J Bacteriol **181**:6306–6311.

49. **Elhai J, Wolk CP**. 1988. Conjugal transfer of DNA to cyanobacteria. Methods Enzymol **167**:747–754.

50. **Olmedo-Verd E, Muro-Pastor AM, Flores E, Herrero A**. 2006. Localized induction of the ntcA regulatory gene in developing heterocysts of *Anabaena* sp. strain PCC 7120. J Bacteriol **188**:6694–6699. http://dx.doi.org/10.1128/JB.00509-06.

51. **Moslavac S, Nicolaisen K, Mirus O, Al Dehni F, Pernil R, Flores E, Maldener I, Schleiff E**. 2007. A TolC-like protein is required for heterocyst development in *Anabaena* sp. strain PCC 7120. J Bacteriol **189**:7887–7895. http://dx.doi.org/10.1128/JB.00750-07.

52. **Pernil R, Picossi S, Mariscal V, Herrero A, Flores E**. 2008. ABC-type amino acid uptake transporters Bgt and N-II of *Anabaena* sp. strain PCC 7120 share an ATPase subunit and are expressed in vegetative cells and heterocysts. Mol Microbiol **67**:1067–1080. http://dx.doi.org/10.1111/j.1365-2958.2008.06107.x.

53. **Missbach S, Weis BL, Martin R, Simm S, Bohnsack MT, Schleiff E**. 2013. 40S ribosome biogenesis co-factors are essential for gametophyte and embryo development. PLoS One **8**:e54084. http://dx.doi.org/10.1371/journal.pone.0054084.

54. **Nicolaisen K, Hahn A, Valdebenito M, Moslavac S, Samborski A, Maldener I, Wilken C, Valladares A, Flores E, Hantke K, Schleiff E**. 2010. The interplay between siderophore secretion and coupled iron and copper transport in the heterocyst-forming cyanobacterium *Anabaena* sp. PCC 7120. Biochim Biophys Acta **1798**:2131–2140. http://dx.doi.org/10.1016/j.bbamem.2010.07.008.

55. **Stevanovic M, Lehmann C, Schleiff E**. 2013. The response of the TonB-dependent transport network in Anabaena sp. PCC 7120 to cell density and metal availability. Biometals **26**:549–560.

56. **Nicolaisen K, Moslavac S, Samborski A, Valdebenito M, Hantke K, Maldener I, Muro-Pastor AM, Flores E, Schleiff E**. 2008. Alr0397 is an outer membrane transporter for the siderophore schizokinen in *Anabaena* sp. strain PCC 7120. J Bacteriol **190**:7500–7507. http://dx.doi.org/10.1128/JB.01062-08.

57. **Oreb M, Zoryan M, Vojta A, Maier UG, Eichacker LA, Schleiff E**. 2007. Phospho-mimicry mutant of atToc33 affects early development of *Arabidopsis thaliana*. FEBS Lett **581**:5945–5951. http://dx.doi.org/10.1016/j.febslet.2007.11.071.

58. **Stevanovic M, Hahn A, Nicolaisen K, Mirus O, Schleiff E**. 2012. The components of the putative iron transport system in the cyanobacterium *Anabaena* sp. PCC 7120. Environ Microbiol **14**:1655–1670. http://dx.doi.org/10.1111/j.1462-2920.2011.02619.x.

59. **Sambrook J, Fritsch E, Maniatis T**. 1989. Molecular cloning: a laboratory manual, 2nd ed. Cold Spring Harbor Laboratory Press, Cold Spring Harbor, NY.

60. **Miyagishima SY, Wolk CP, Osteryoung KW**. 2005. Identification of cyanobacterial cell division genes by comparative and mutational analyses. Mol Microbiol **56**:126–143. http://dx.doi.org/10.1111/j.1365-2958.2005.04548.x.

61. **Karimova G, Dautin N, Ladant D**. 2005. Interaction network among *Escherichia coli* membrane proteins involved in cell division as revealed by bacterial two-hybrid analysis. J Bacteriol **187**:2233–2243. http://dx.doi.org/10.1128/JB.187.7.2233-2243.2005.

62. **Cserzö M, Wallin E, Simon I, von Heijne G, Elofsson A**. 1997. Prediction of transmembrane alpha-helices in prokaryotic membrane proteins: the dense alignment surface method. Protein Eng **10**:673–676. http://dx.doi.org/10.1093/protein/10.6.673.

63. **Jones DT, Taylor WR, Thornton JM**. 1994. A model recognition approach to the prediction of all-helical membrane protein structure and topology. Biochemistry **33**:3038–3049. http://dx.doi.org/10.1021/bi00176a037.

64. **Hofman K, Stoffel W**. 1993. TMbase—a database of membrane spanning proteins segments. Biol Chem **374**:166.

65. **Mitaku S, Hirokawa T, Tsuji T**. 2002. Amphiphilicity index of polar amino acids as an aid in the characterization of amino acid preference at membrane-water interfaces. BioInformatics **18**:608–616. http://dx.doi.org/10.1093/bioinformatics/18.4.608.

66. **Juretić D, Zoranić L, Zucić D**. 2002. Basic charge clusters and predictions of membrane protein topology. J Chem Inf Comput Sci **42**:620–632.

67. **Cao B, Porollo A, Adamczak R, Jarrell M, Meller J**. 2006. Enhanced recognition of protein transmembrane domains with prediction-based structural profiles. Bioinformatics **22**:303–309. http://dx.doi.org/10.1093/bioinformatics/bti784.

68. **Deber CM, Wang C, Liu LP, Prior AS, Agrawal S, Muskat BL, Cuticchia AJ**. 2001. TM finder: a prediction program for transmembrane protein segments using a combination of hydrophobicity and nonpolar phase helicity scales. Protein Sci **10**:212–219. http://dx.doi.org/10.1110/ps.30301.

69. **Bernsel A, Viklund H, Hennerdal A, Elofsson A**. 2009. TOPCONS: consensus prediction of membrane protein topology. Nucleic Acids Res **37**:W465–W468. http://dx.doi.org/10.1093/nar/gkp363.

70. **Rost B, Casadio R, Fariselli P, Sander C**. 1995. Transmembrane helices predicted at 95% accuracy. Protein Sci **4**:521–533. http://dx.doi.org/10.1002/pro.5560040318.

71. **Krogh A, Larsson B, von Heijne G, Sonnhammer EL**. 2001. Predicting transmembrane protein topology with a hidden Markov model: application to complete genomes. J Mol Biol **305**:567–580. http://dx.doi.org/10.1006/jmbi.2000.4315.

72. **Mariscal V, Herrero A, Nenninger A, Mullineaux CW, Flores E**. 2011. Functional dissection of the three-domain SepJ protein joining the cells in cyanobacterial trichomes. Mol Microbiol **79**:1077–1088. http://dx.doi.org/10.1111/j.1365-2958.2010.07508.x.